Biol. Cybern. 82, 161–172 (2000)

Biological Cybernetics

Investigating centre of mass stabilisation as the goal of posture and movement coordination during human whole body reaching

Paul Stapley[1], **Thierry Pozzo**[1], **Alexander Grishin**[2], **Charalambos Papaxanthis**[1]

[1] Groupe d'Analyse du Mouvement (GAM), UFR STAPS BP 27877, Université de Bourgogne, F-21078 Dijon, Cedex, France
[2] Institute for Information Transmission Problems, Russian Academy of Sciences, B. Karenty per 19 GSP-4, Moscow, Russia

Received: 22 September 1998 / Accepted in revised form: 2 June 1999

Abstract. In the light of experimental results showing significant forward centre of mass (CoM) displacements within the base of support, this study investigated if whole body reaching movements can be executed whilst keeping the CoM fixed in the horizontal axis. Using kinematic simulation techniques, angular configurations were recreated from experimental data imposing two constraints: a constant horizontal position of the CoM and an identical trajectory of the hand to grasp an object. The comparison between recorded and simulated trials showed that stabilisation of the CoM was associated with greater backward hip displacements, which became more marked with increasing object distance. This was in contrast to recorded trials showing reductions in backward hip displacements with increasing distance. Results also showed that modifications to angular displacements were necessary only at the shoulder and hip joints, but that these modifications were within the limits of joint mobility. The analysis of individual joint torques revealed that the pattern and timing of simulated trials were similar to those recorded experimentally. Peak joint torque values showed particularly that keeping the CoM at a constant horizontal position resulted in significantly smaller ankle peak flexor and extensor torques. It may be concluded from this study that 'stabilising' the CoM during human whole body reaching represents a feasible strategy, but not the one chosen by subjects under experimental conditions. Our results also do not support the idea of the CoM as the stabilised reference value for the coordination between posture and goal-directed movements.

Correspondence to: P. Stapley,
Neurological Sciences Institute,
Oregon Health Sciences University,
1120 NW 20th Ave, Portland, OR 97209,
USA

1 Introduction

1.1 The whole body centre of mass: a stabilised reference for posture and movement coordination

Previous studies (Crenna et al. 1987; Oddsson 1988; Oddsson and Thortensson 1986; Pedotti et al. 1989), and more recently Alexandrov et al. (1998), have shown that during forward and backward trunk bending movements, the body centre of mass (CoM) is efficiently regulated with respect to the base of support (BoS). Horizontal CoM displacements were reduced to amplitudes as low as 1.4 cm by what these authors termed 'axial synergies', described as opposing displacements of trunk and knee segments with those of the hips (originally documented by Babinski 1899). Such axial synergies have also been shown to minimise CoM displacements during trunk bending movements executed under microgravity conditions (Massion et al. 1997), suggesting an invariance of the horizontal CoM position with respect to the supporting surface. The idea of the CoM as the stabilised reference value for posture and movement coordination (see Massion 1992) has been adopted by other authors investigating a range of whole body movements executed, for example, with changing BoS configurations (Mouchnino et al. 1992; Nardone and Schiepatti 1988), different moving segments (Bouisset and Zattara 1981; Eng et al. 1992), or during altered environmental conditions (Horstmann and Dietz 1990; Mouchnino et al. 1996).

1.2 CoM control during multi-joint goal-directed reaching movements

Results from experiments of goal-directed reaching movements have led to some doubt concerning the stabilisation of the body CoM. Tyler and Hazan (1995), studying arm reaching movements in the sitting position, compared muscle torques simulated with the trunk stable and abdominal and paraspinal electromyographic (EMG) activity from recorded movements (trunk free). Their findings showed that for some movement direc-

tions, recorded EMG signals did not match simulated trunk torques, suggesting that the central nervous system (CNS) does not consistently program muscular activity to resist trunk (and therefore CoM) motion.

In a recent study (Stapley et al. 1998), we have re-examined postural adjustments associated with voluntary whole body reaching movements executed from the standing posture. During this task, despite compensatory or 'axial' synergies of the trunk and hips, CoM displacements showed horizontal amplitudes of up to 0.112 m (80.4% of relative BoS length). These amplitudes exceeded those of a study by Ramos and Stark (1990b), who simulated forward trunk bending movements without backward hip displacements. The essential findings of our study were, however, that anticipatory postural adjustments (APAs) in the muscles of the lower limb (soleus and tibialis anterior) preceding whole body reaching created the necessary dynamic conditions for forward displacements of the CoM within the BoS. A postural role of anticipatory muscular activity has been suggested for a wide range of arm movements executed from the standing posture (Belenkii et al. 1967; Bouisset and Zattara 1981; Cordo and Nashner 1982; Friedli et al. 1984; Lee et al. 1987). The widely accepted theory is that such APAs act to resist disturbances induced by the focal aspects of the movement (Bouisset and Zattara 1981, 1987), without which the body would invariably fall over (Ramos and Stark 1990a). Our results suggested, however, that what has previously been classified as postural muscular activity can also serve a focal role of whole body displacement in a forward direction.

1.3 Aims of the present study

Our previous results have shown that during whole body reaching movements, APAs create the necessary conditions for forward CoM displacement, and despite the presence of similar axial strategies, horizontal CoM amplitudes exceed those of other forward trunk bending movements. Based upon these preliminary results, the present study aimed to study in greater detail if the CoM indeed represents the stabilised reference value during human whole body reaching. Any experimental findings confirming large horizontal CoM amplitudes under different reaching conditions would suggest either that subjects cannot execute such a task whilst stabilising the CoM, or that CoM displacement represents a solution adopted by the CNS. To this end, the present study will investigate, through kinematic simulation, if it is indeed possible to execute whole body reaching movements when the CoM remains at a constant coordinate in the horizontal (x) axis.

2 Materials and methods

2.1 Description of the whole body reaching task

Six healthy subjects (four males and two females, aged 18–35 years, mean height 1.71 ± 0.06 m, mean mass 69.1 ± 9.2 kg (678.8 ± 91.1 N), mean foot size 0.255 ± 0.064 m, participated in the study. From an initial standing posture with the arms in front of the body, the two hands crossed left over right at the level of the navel, subjects were asked to reach and lift an object (0.40 m long, 0.07 m in diameter and 1.8 kg in mass), to shoulder height. No indications as to the strategy required to reach the object were given. All subjects used a strategy of coordinated trunk, hip, knee and ankle flexion to reach the target. Each subject grasped the object from above using an open-fisted cylindrical grip. Trials were divided into two blocks of reach to lift movements, each separated by a rest period of approximately 3 min. The first block consisted of five trials executed with the object placed at a distance of 5% of each subject's height (D1). The second block consisted of a further five trials with the object at 30% height (D2). Each subject thus executed a total of ten trials, all at naturally paced speed. During a practice period, subjects were asked to execute reach-to-lift movements twice at each distance (four trials).

2.2 Apparatus

Two cameras (sampling frequency 100 Hz), each placed 3 m from the subject's sagittal axes, one above the other 1 m and 2 m from the ground, recorded movements of retro-reflective markers (15 mm in diameter), glued to 11 anatomical sites, using an optoelectronic measuring device ELITE (BTS, Milan, Italy). The 11 markers were placed on each subject's left side at the following sites: the external canthus of the eye, the auditory meatus of the ear, at the level of the inferior angle of the omoplate and at the vertical of the axil, the greater trochanter, the knee interstitial joint space, the external malleolus, the fifth metatarsophalangeal, the acromial process of the shoulder, the lateral condyle of the elbow, the wrist styloid process and the fifth metacarpophalangeal. Horizontal (F_X), vertical (F_Z) and mediolateral (F_Y) ground reaction forces and the position of the centre of foot pressure (CoP) were obtained using an AMTI (Advanced Mechanical Technology Inc. Watertown, USA) force platform (sampling frequency 500 Hz). Surface EMG signals were recorded from four pairs of antagonistic muscles (see Stapley et al. 1998), but are not reported here.

Acquisitions began at least 1 s before a tone signal upon which subjects were instructed to reach, and ended 1 s after lift termination. Intentional (focal) movement onset (t_0) was determined using curvilinear velocity profiles of the wrist marker. Onsets were defined in the first instance as the first 10-ms period where wrist velocity profiles showed sustained deflections above zero. Verifications were made whereby onsets and offsets were considered valid only if they exceeded a threshold of 5% maximum velocity. Furthermore, onsets (and offsets) were accepted only if they preceded peak velocities greater than 30% of maximum values recorded for each segment during the reaching phase. Thus, for each trial, t_0 was defined as the time at which wrist curvilinear displacements began.

2.3 Data analysis

Total amplitudes of head, shoulder, wrist, hip and knee segments were calculated along the horizontal (x) axis during the reaching phase. Shoulder, hip, knee and ankle inter-segmental joint angles were computed in a counter-clockwise direction using the following segments: (1) shoulder, the angle from the upper arm to the upper trunk segment; (2) hip, the angle from the thigh to the abdomen-pelvis segment; (3) knee, the angle from the shank to the thigh segment; (4) ankle, the angle from shank to the foot. Angles in flexion were characterised by backward motion of the upper arm relative to the upper trunk (shoulder flexion), forward motion of the upper trunk relative to the thigh (hip flexion), the thigh backwards and downwards relative to the shank (knee flexion) and a forwards motion of the shank relative to the *foot* (ankle dorsi-flexion). Angles in extension were determined between the same segments used for shoulder, hip, knee and ankle flexion, but in an opposite direction. The orientation angle of the whole trunk (upper trunk and abdomen-pelvis segments), with respect to the vertical (positive in a counter-clockwise direction) was also calculated. This was taken as the angle made by the main axis of the segment joining hip and shoulder markers.

2.4 CoM and joint torque calculations

Sagittal whole body CoM positions were calculated using a seven-segment, rigid mathematical model consisting of the following appendicular and axial body segments: head-neck, upper trunk, abdomen-pelvis, thigh, shank, upper arm and forearm. Positions of segment ends were obtained from recorded horizontal and vertical displacement values. Using the model, the position of the CoM of an ith segment with co-ordinates X_i, Z_i was calculated using the following formulae:

$$X_i = X1_i + l_i(X2_i - X1_i) \text{ and } Z_i = Z1_i + l_i(Z2_i - Z1_i) \ , \quad (1)$$

where $X1_i, Z1_i, X2_i, Z2_i$ = coordinates of segment ends, l_i = the ratio between the distance of the proximal marker to the segments CoM, and its length. Coordinates in X and Z of the whole body CoM were thus calculated using the formulae:

$$X = \sum m_i X_i / \sum m_i \text{ and } Z = \sum m_i Z_i / \sum m_i \ , \quad (2)$$

m_i being the mass of the ith segment. Anthropometric parameters including segment masses, moments of gyration and positions of their individual centres of mass were taken from Plagenhoef et al. (1983). The trunk was divided in two at the L5-S1 level to optimise the determination of the whole body CoM (see Kingma et al. 1995).

Three separate CoM calculations were made in order to evaluate the effectiveness of upper and lower body segments in offsetting overall whole body CoM displacements. The calculation of the whole body CoM is outlined above. The second or upper body CoM (CoMu) was calculated using segments of the upper trunk (thorax), head-neck, upper arm and forearm. The third lower body CoM (CoMl) consisted of abdomen-pelvis, thigh, shank and foot segments.

Anthropometric parameters, including segment masses, moments of inertia and positions of their individual CoM, were used to determine segment CoM positions, as well as net torques and forces acted upon each of the joints. The model was considered as an open loop kinematic chain, applying Newton-Euler equations of motion to the observed motion of any one-joint segment. By systematically considering one segment at a time, equations for force and torque were:

$$m_i \vec{a}_i = \sum_j \vec{F}_{ij} + m_i \vec{g} \quad (3)$$

$$J_i \dot{\omega}_i \vec{y} = \sum_i \left[M_{ij} \left(\vec{O}_j \right) + \vec{F}_{ij} \, x \, \vec{e}_j \right] \quad \text{with}$$

$$\vec{e}_j = \vec{O}_j \vec{G}_j \ , \quad (4)$$

where $\vec{F}_{ij}, M_{ij} =$ vectors of force and scalar torque acted upon joint j of the segment i, respectively. m_i, J_i, a_i, $\dot{\omega}_i$ represent segment mass, its moment of gyration relative to the CoM, a vector of CoM acceleration, and angular acceleration of the segment around an axis perpendicular to the plane of motion, respectively. A segments' CoM acceleration a_i and its angular acceleration $\dot{\omega}_i$ were calculated using X and Z coordinates, its length and accelerations of proximal and distal ends.

2.5 Kinematic simulation procedures

The purpose of the kinematic simulation was to reconstruct new trajectories of all body segments in order that the initial position of the CoM should be fixed whilst conserving recorded wrist marker trajectories. Experimental wrist marker trajectories were used during kinematic simulation procedures in order to conserve a degree of ecological validity (simulated trials were compatible with object grasp). Movements were considered in the sagittal plane only. To achieve simulation procedures, Fig. 1 illustrates a rigid six-segment model (different from the seven-segment model used for CoM calculation; see Sect. 2.4) comprising the following segments: upper body, ub (head-neck and upper trunk segments), lower body, lb (abdomen-pelvis), thigh (th), shank (sh), upper arm (ua) and forearm (fa). The foot segment was eliminated from the simulation model and ankle marker coordinates remained constant. The configuration of segments in Fig. 1 was represented by six angles, four vertical (Z) spatial angles $\theta_1, \theta_2, \theta_3, \theta_5$ comprising th, sh, lb and ua segments, and two inter-segmental angles θ_4, θ_6 between ub and lb, and fa and ua segments, respectively. Angles used in simulation procedures were different from those used to quantify differences between recorded and simulated trials (see

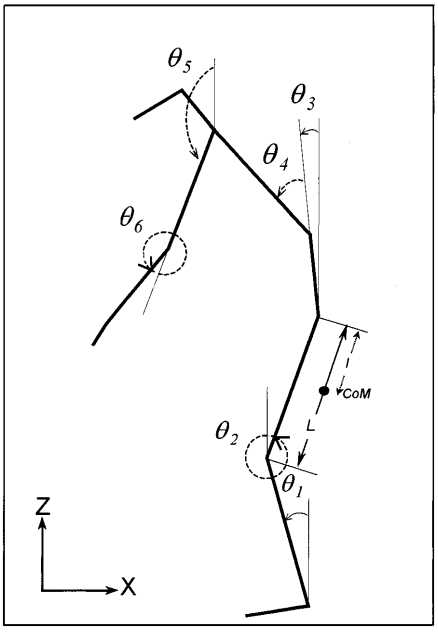

Fig. 1. Simplified six-segment model used for kinematic simulation procedures. Shown are four limb spatial angles with respect to the vertical $\theta_1, \theta_2, \theta_3, \theta_5$ and two inter-segmental angles θ_4, θ_6. Also shown is L (segments length) and l (the distance between a segment's distal end and its centre of mass)

Sect. 2.3). Each segment used in the model was represented by its mass m, length L, and distance l (between the segments distal end and its centre of mass). Each segment mass and positions of the segments' CoM were calculated using documented anthropometric parameters (Plagenhoef et al. 1983). Wrist marker coordinates ($X_{\mathrm{wr}}, Z_{\mathrm{wr}}$) and the horizontal location of the CoM at the instant of intentional movement onset (t_0) were obtained using the following formulae;

$$X_{\mathrm{wr}} = -L_{\mathrm{sh}}\sin\theta_1 - L_{\mathrm{th}}\sin\theta_2 - L_{\mathrm{lb}}\sin\theta_3 - L_{\mathrm{ub}}\sin(\theta_3+\theta_4) - L_{\mathrm{ua}}\sin\theta_5 - L_{\mathrm{fa}}\sin(\theta_5+\theta_6) \ ,$$

$$Z_{\mathrm{wr}} = L_{\mathrm{sh}}\cos\theta_1 + L_{\mathrm{th}}\cos\theta_2 + L_{\mathrm{lb}}\cos\theta_3 + L_{\mathrm{ub}}\cos(\theta_3+\theta_4) + L_{\mathrm{ua}}\cos\theta_5 + L_{\mathrm{fa}}\cos(\theta_5+\theta_6) \ ,$$

$$\begin{aligned} X_{\mathrm{CM}} = -\{&[l_{\mathrm{sh}}m_{\mathrm{sh}} + L_{\mathrm{sh}}(m_{\mathrm{th}}+m_{\mathrm{lb}}+m_{\mathrm{ub}}+m_{\mathrm{ua}}+m_{\mathrm{fa}})]\sin\theta_1 \\ &+ [l_{\mathrm{th}}m_{\mathrm{th}} + L_{\mathrm{th}}(m_{\mathrm{lb}}+m_{\mathrm{ub}}+m_{\mathrm{ua}}+m_{\mathrm{fa}})]\sin\theta_2 \\ &+ [l_{\mathrm{lb}}m_{\mathrm{lb}} + L_{\mathrm{lb}}(m_{\mathrm{ub}}+m_{\mathrm{ua}}+m_{\mathrm{fa}})]\sin\theta_3 \\ &+ [l_{\mathrm{ub}}m_{\mathrm{ub}} + L_{\mathrm{ub}}(m_{\mathrm{ua}}+m_{\mathrm{fa}})]\sin(\theta_3+\theta_4) \\ &+ [(L_{\mathrm{ua}}-l_{\mathrm{ua}})m_{\mathrm{ua}} + L_{\mathrm{ua}}m_{\mathrm{fa}}]\sin\theta_5 \\ &+ (L_{\mathrm{fa}}-l_{\mathrm{fa}})m_{\mathrm{fa}}\sin(\theta_5+\theta_6)\}/M \ , \end{aligned} \tag{5}$$

where M represents the sum of the masses of all segments. Demands placed upon the conservation of recorded wrist trajectories and a constant X position of the CoM, led to the following equations:

$$\begin{cases} X_{\mathrm{wr}} = \tilde{X}_{\mathrm{wr}} \\ Z_{\mathrm{wr}} = \tilde{Z}_{\mathrm{wr}} \\ X_{CM} = X_0 \ , \end{cases} \tag{6}$$

where $\tilde{X}_{\mathrm{wr}}, \tilde{Z}_{\mathrm{wr}}$ are recorded wrist coordinates and X_0 is the initial CoM position. The system (5) imposes three equations upon the six known angles θ_{1-6}. To calculate a unique solution, a least-squares fitting technique was used. The set of angles θ_{1-6} were recalculated so as to satisfy (6) but remain as close as possible to recorded values $\tilde{\theta}$, thus supplying a minimum value to the square function S:

$$S = \sum_{j=1}^{6} (\theta_j - \tilde{\theta}_j)^2 \ . \tag{7}$$

Solutions to task (7) are as described in Appendix 1. Following kinematic simulation procedures, segment displacements, angles in flexion and extension, individual joint torques, as well as whole body and partial CoM displacements were recalculated for files possessing the 'new' geometry. Simulated horizontal CoP displacements relative to the centre of ankle joint (X_{CoP}) were calculated using the following formula:

$$X_{\mathrm{CoP}} = M_{\mathrm{A}}/Fz \ , \tag{8}$$

where M_{A} is the simulated ankle torque and Fz the simulated vertical component of ground reaction forces.

The present study will report results from a total of four conditions. D1E and D2E are the two experimental (E) conditions of differing reaching distance. Simulated (S) movements of angular configurations reconstructed from experimental data gave a further two conditions (D1S and D2S). Main effect differences between dependent variables were tested using a 2×2 (two distances, D1 and D2 under two conditions, E and S) multivariate analysis of variance (MANOVA). Post hoc analysis was conducted using a Neuman-Keuls test. A Kolmogorov-Smirnov test of normality was also used to test for the existence of a normal data distribution.

3 Results

3.1 Sagittal body kinematics

Figure 2 illustrates separate CoM trajectories (averages of four trials for each subject) during experimental and simulated whole body reaching movements. In experimental trials (at both distances), despite opposing displacements of head, shoulder, wrist and knee segments with those of the hip, the CoM showed initial forward, followed by downward vertical and continuing forward horizontal trajectories until object grasp. Table 1 lists averaged horizontal CoM displacements of experimental trials, whose values represented 33.4 ± 13.6% and 63.9 ± 16.5% of relative BoS length for D1E and D2E, respectively.

Forward and downward CoM trajectories of experimental trials were accompanied by CoMu trajectories of similar form. CoMl trajectories revealed initial back-

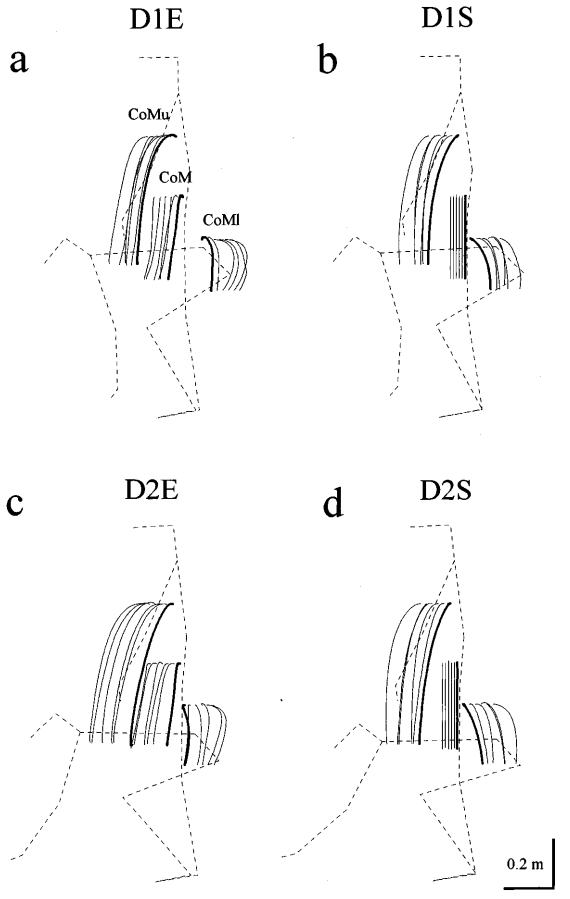

Fig. 2a–b. Whole (*CoM*), upper (*CoMu*) and lower (*CoMl*) body centre of mass trajectories during experimental and simulated trials at both distances. Each trajectory represents the mean of four trials for each of the six subjects. *Thicker trajectories* indicate averages for the subject corresponding to the stick figures. Trajectories have been normalised in amplitude. For clarity, CoM and CoMu trajectories have been displaced by 20 mm in the direction of movement (forwards), with those of the CoMl being displaced 20 mm in the direction opposite to that of the movement (backwards). Conditions are: D1E (distance 1, experimental), D1S (distance 1, simulated), D2E (distance 2, experimental) and D2S (distance 2, simulated)

ward displacements opposite in polarity to those of the CoM and CoMu (Fig. 2A, C). Approximately midway through reaching, however, recorded CoMl trajectories became oriented in a direction similar to those of the CoM and CoMu. Simulated CoM trajectories revealed quite a different pattern. Keeping the X coordinates of the CoM constant produced clear opposing displacements of upper (CoMu) and lower (CoMl) body segments (Fig. 2B,D). There was also no forward directed trajectory of the CoMl in simulated trials (as seen to occur in recorded reaching movements). Table 2 lists average horizontal displacements of whole, upper and lower body CoM for all subjects under experimental and simulated conditions. Keeping the CoM horizontally fixed at both reaching distances led to significantly reduced forward CoMu horizontal amplitudes ($P < 0.001$), and greater backward CoMl amplitudes ($P < 0.001$).

Figure 3 shows general characteristics of whole body reaching movements at both distances and under experimental and simulated conditions. In experimental trials, increases in horizontal wrist marker displacements with distance were accompanied by corresponding increases in shoulder and knee forward displacements, whereas head segment displacements remained unchanged. An important finding from experimental trials, particularly evident in Fig. 3, was that the hip showed significantly reduced backward displacements when reaching distance increased ($P < 0.001$). Figure 3 also shows that under simulated compared to experimental conditions, there were marked reductions in horizontal head, shoulder and knee forward displacements at both distances, with decreases being most evident at D2. It is important to note, however, that with stabilised strategies, the hip was displaced further backwards at both D1 ($P < 0.001$) and D2 ($P < 0.001$). Average horizontal head, shoulder, wrist, knee and hip displacements for all subjects and conditions are presented in Fig. 4.

3.2 Body geometry

Figure 5 shows average angular displacements of shoulder, hip, knee and ankle joints under all conditions. Generally, in experimental trials, regardless of distance, largest intersegmental angular displacements occurred at the knee and hip, followed by the shoulder and ankle. As reaching distance increased, significantly greater recorded angular displacements were produced at the knee ($P < 0.001$) and shoulder ($P < 0.001$), but not at the hip or ankle ($P > 0.05$).

Figure 5C shows that knee angular displacements remained relatively unchanged between experimental and

Table 1. Average horizontal displacements of whole (*CoM*), upper (*CoMu*) and lower (*CoMl*) body centres of mass for all subjects at both distances, in recorded and simulated conditions. + = forward displacements, – = backward displacements. Units are shown in metres. It should be noted that in simulated conditions, there is no forward displacement of either CoM or CoMl

Centre of mass		Horizontal displacement (m)			
		D1E	D1S	D2E	D2S
Whole body (CoM)	+	0.050 (0.020)	–	0.091 (0.021)	–
Upper body (CoMu)	+	0.138 (0.024)	0.09 (0.013)	0.189 (0.026)	0.10 (0.012)
Lower body (CoM1)	–	0.039 (0.018)	0.063 (0.009)	0.019 (0.016)	0.075 (0.008)
	+	0.048 (0.007)	–	0.023 (0.011)	–

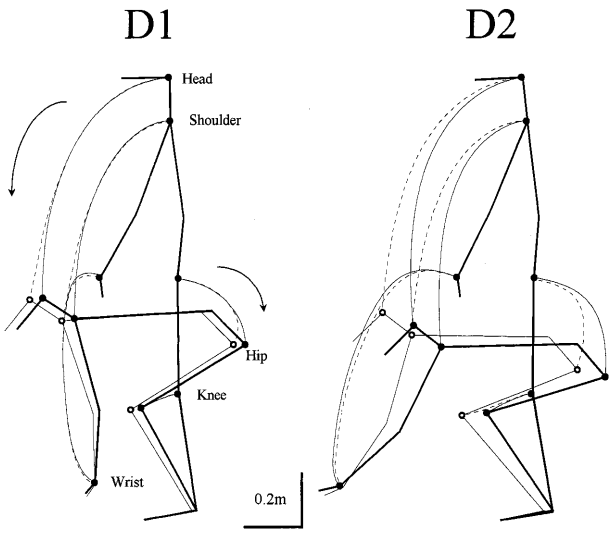

Fig. 3. General characteristics of whole body reaching. Sagittal plane segment trajectories during experimental and simulated reaching movements made to objects placed at 5% (D1) and 30% (D2) of each subjects height. Stick figure positions and trajectories represent averages of four trials (one subject, S5). Experimentally recorded trials are shown as *thin sticks* and *dashed* trajectories, and simulated trials as *bold sticks* and *thin full* trajectories. *Open* (recorded trials) and *filled circles* (simulated trials) indicate initial and final positions of head, shoulder, wrist, hip and knee markers

simulated conditions. There were also insignificant decreases ($P > 0.05$) in ankle angular displacements during simulated reaching at both distances, (see Fig. 5D). There were however, significant increases in shoulder extension ($P < 0.001$) and hip flexion ($P < 0.001$) at D2 during simulated trials. Mean shoulder angles increased from 75.8 ± 6.7° (D2E) to 91.5 ± 10° (D2S), and the hip from 99 ± 12° (D2E) to 111.7 ± 16.9° (D2S). The in-

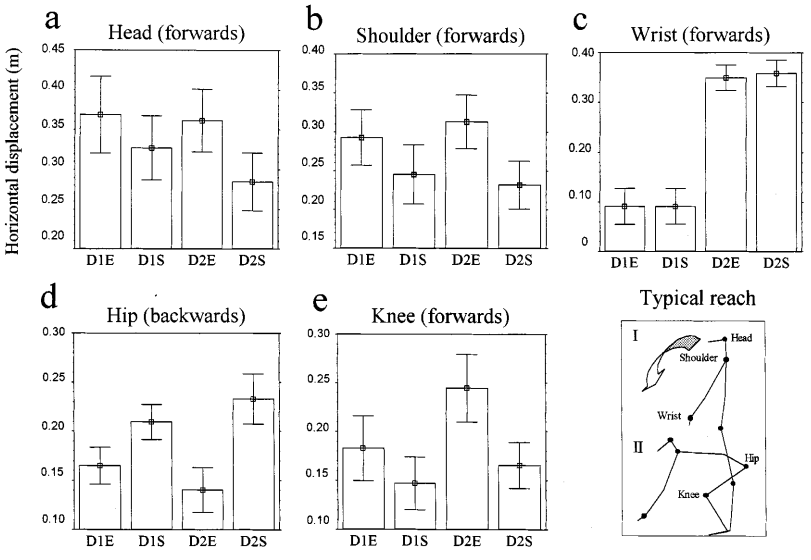

Fig. 4a–e. Means (plus and minus one standard deviation) of horizontal amplitudes of head, shoulder, wrist, hip and knee markers. *Inset* shows stick-figure representations of first (I) and last (II) frames of one representative reach (subject 3, D2), between which amplitudes were calculated, as well as locations of head, shoulder, wrist, hip, and knee segments

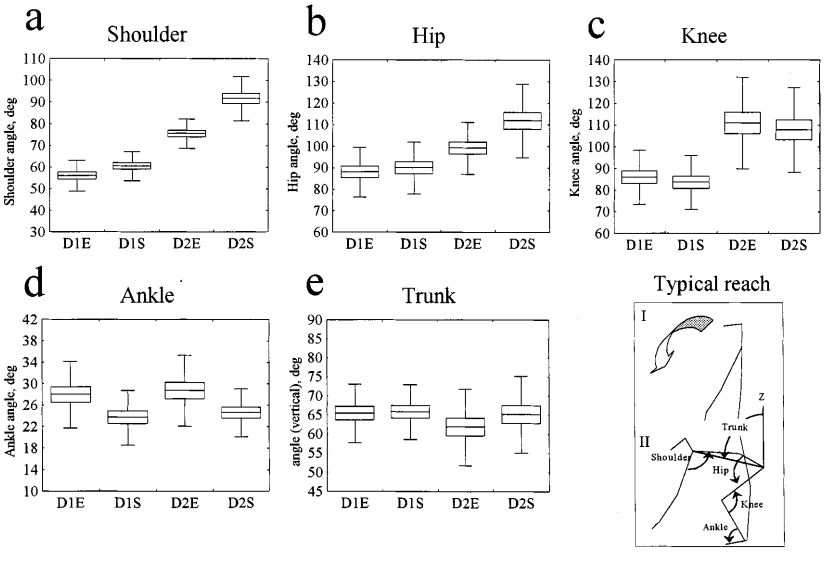

Fig. 5a–e. Angular displacements of shoulder, hip, knee and ankle joints measured between initial standing postures and the end of reaching **e** shows trunk angular displacements with respect to the vertical (Z) axis. Values represent averages of all six subjects in each of the four conditions. Mean values correspond to *horizontal lines within the rectangles*; plus and minus one standard error of the mean to the *top and bottom of the rectangles*; and 95th and 5th percentiles, to the *upper and lower limits of the I-bar*. *Inset* shows stick-figure representations of first (I) and last (II) frames of one representative reach (subject 3, D2), the four intersegmental (shoulder, hip, knee and ankle) angles and the trunk orientation angle with respect to the vertical (Z). The four conditions are as described in Fig. 2

Table 2. Timing of peak flexor and extensor torques for the shoulder, hip, knee and ankle as a percentage of the reaching phase

Joint torque	Percentage of reaching movement time (%)			
	D1E	D1S	D2E	D2S
Shoulder flexion	77.5 (13.9)	71.2 (12.1)	56.7 (7.9)	48.2 (13.3)
Shoulder extension	30.4 (20.2)	18.2 (15.1)	82.5 (15.3)	95.9 (3.4)
Hip flexion	14.9 (6.7)	13.9 (6.6)	16.3 (7.2)	15.9 (10)
Hip extension	95.7 (6.8)	94.8 (6.9)	95.9 (5.9)	88.9 (8.8)
Knee flexion	94.2 (9.2)	94.5 (8.3)	97.3 (8.4)	94.6 (7.9)
Ankle flexion	30.1 (6.4)	33 (6.9)	44.6 (13.6)	34.9 (5.7)
Ankle extension	96 (4.2)	92.6 (14.3)	95.5 (5.7)	85.1 (14.5)

crease of on average 15.7° in shoulder extension probably arose as a result of greater object placement distance. The greater hip flexion associated with CoM stabilisation at D2 resulted from increased backward hip displacements (Fig. 4D). This is upheld by findings of both decreased knee forward displacements (Fig. 4E) coupled with unchanged trunk angular displacements with respect to the vertical across all four conditions (see Fig. 5E). Vertical trunk angular displacements ranged from 61.8 ±10° (D2E) to 65.7 ±7.1° (D1S).

3.3 Net joint torques

Figure 6 shows that hip, knee and ankle net joint torques showed initial flexion (although slight at the hip) at both reaching distances. During the second half of the reaching phase, hip, knee and ankle joints demonstrated extensor torques. Shoulder torques modified as a function of object distance: peak flexion occurred earlier at D2, ending with larger extensor torques. The general pattern and timing of net joint torque profiles in simulated trials remained similar to those recorded experimentally (Fig. 6). Table 2 lists times to peak flexion and extension relative to the total reaching movement time.

Figure 7 shows that during experimental trials, highest values of peak flexor torques were exerted at the ankle, followed by the hip and shoulder. Significant increases in peak hip net flexor torques occurred experimentally with increasing distance ($P < 0.01$). Probably as a result of increasing object distance, shoulder flexion decreased when subjects reached at D2. Increases in recorded ankle peak flexor torques with distance failed to reach significance ($P > 0.05$). Peak extensor torques towards the end of the reaching phase showed significant increases in experimental trials between D1 and D2, at all joints (shoulder, $P < 0.001$; hip, $P < 0.01$; knee, $P < 0.01$; ankle, $P < 0.01$).

The simulation of constant horizontal CoM coordinates led to modifications in the distribution of the net joint torque in the four joints studied. Figure 7 shows that in hip and ankle joints, there were decreases in initial peak flexor torques at both distances (hip, $P < 0.05$; ankle, $P < 0.001$), but significant increases in knee flexor torques ($P < 0.01$), compared to experimental data. As can be seen from Fig. 7, CoM stabilisation resulted in unchanged hip extensor torques at both distances ($P > 0.05$), as well as the shoulder at D1.

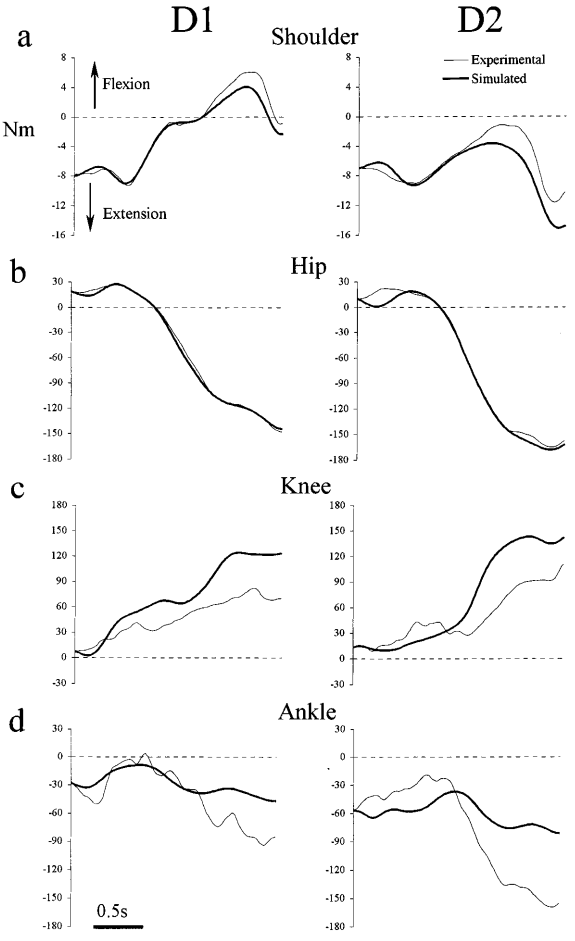

Fig. 6 a–d. General trends of net joint torques in the four joints studied; shoulder, hip, knee and ankle for both distance conditions. Experimental trials are shown as thin lines and simulated trials thick lines. Data are taken from one typical subject, from the beginning to the end of reaching

The shoulder extensor torques did, however, significantly increase with distance ($P < 0.05$). An important finding was large decreases in ankle extensor torques at both distances under simulated compared to experimental conditions ($P < 0.001$).

3.4 Centre of pressure displacements

Figure 8A shows that in experimental trials there were three distinct phases to CoP displacements; an initial backward displacement, after which the CoP passed in

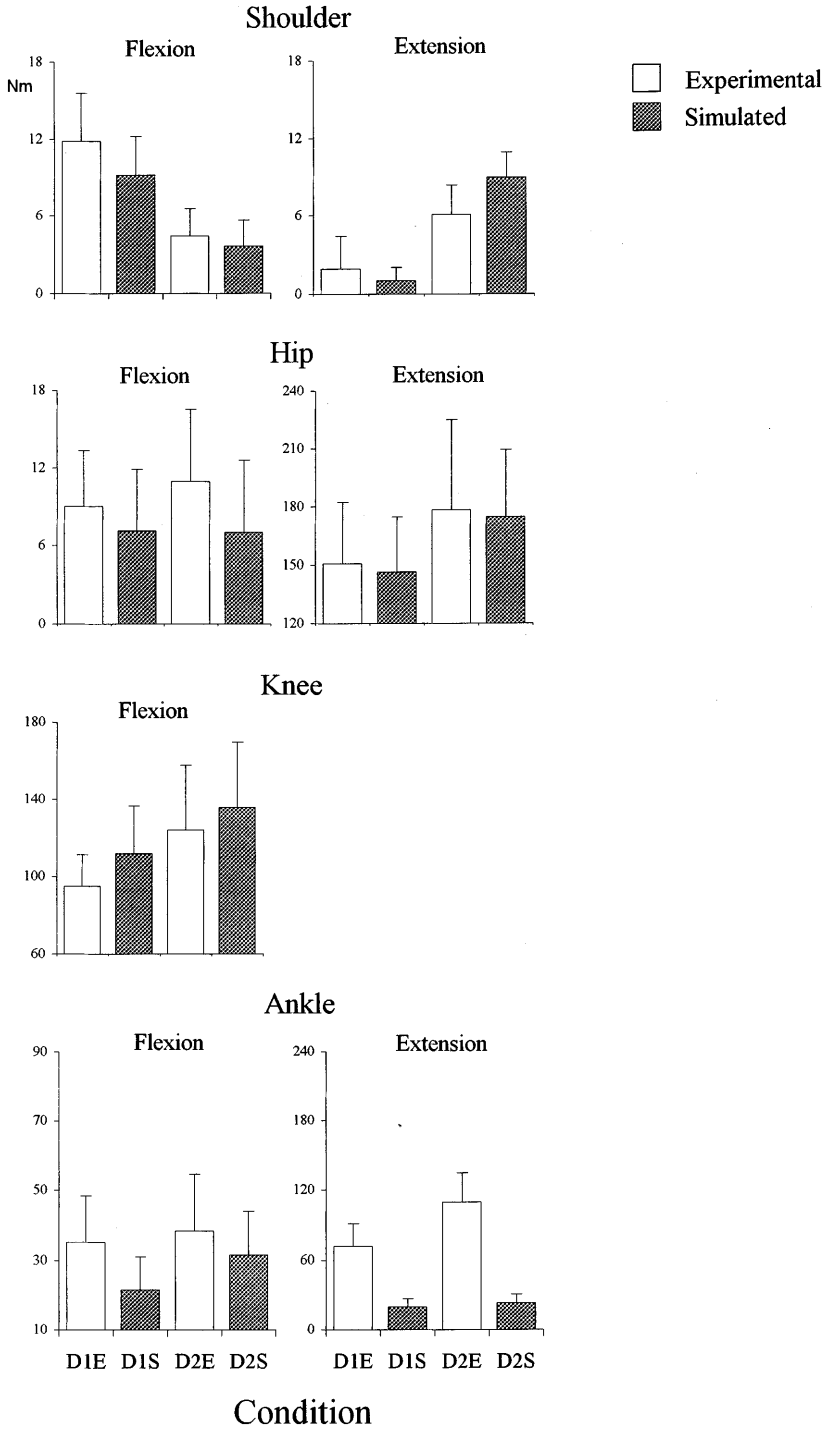

Fig. 7. Mean peak shoulder, hip, knee and ankle joint torques in flexion (*left*) and extension (*right*) for all subjects and trials. *Open bars* Experimental trials, *shaded bars* simulated trials. Conditions are as described in Fig. 2

front of the CoM and finished at the anterior limit of the BoS (at the end of reaching). Estimated CoP displacements from simulated trials demonstrated similar trends to experimental ones, except that both backward and forward peak amplitudes were significantly reduced and CoP displacements terminated close to the CoM. In experimentally recorded trials, initial positions of the CoP corresponded to 33.5 ±14.1% (D1E) and 43.2 ±17.2% (D2E) of the relative foot length. Figure 8B illustrates increases in initial backward and forward CoP displacements experimentally with greater reaching distance (backwards, $P < 0.001$, forwards, $P < 0.01$), with forward CoP shifts reaching the very anterior limits of the BoS. Ranges of reconstructed CoP displacements for simulated trials were greatly reduced compared to experimental trials. There were significant main effects of conditions for both backward ($P < 0.001$) and forward ($P < 0.001$) peak CoP displacements at both distances. These results indicate that keeping the CoM constant along the x-axis was compatible with dynamic equilibrium constraints (the CoP did not leave the supporting foot area).

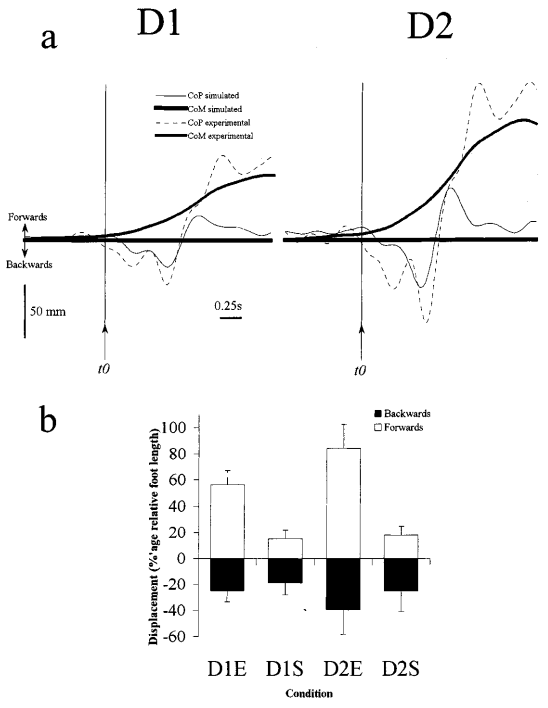

Fig. 8. **a** Experimental and simulated horizontal centre of mass (*CoM*) and centre of pressure (*CoP*) displacements for a typical trial at each distance (one subject). **b** All subject (average) amplitudes of CoP displacements expressed as a percentage of the distance between markers placed at the 5th metatarsophalangeal and the external malleolus of each subjects left foot. 0 corresponds to the initial CoP position between these two markers (D1 = 33.5%, D2 = 43.2%). Conditions are as described in Fig. 2

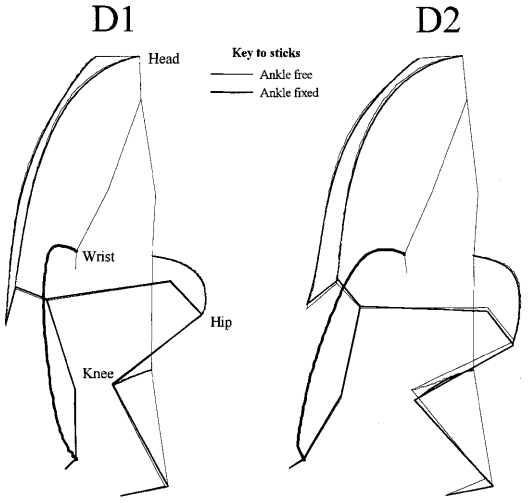

Fig. 9. A comparison between recorded whole body reaching (where the ankle marker was free to move) and simulations that involved fixing the ankle and conserving an identical wrist trajectory. Recorded movements are represented by *thin sticks* and simulated ones *darker sticks*. Also shown are head (the Francfort plane), hip, knee and wrist trajectories (recorded trajectories = *thin lines*, simulated trajectories = *thicker lines*)

4 Discussion

Simulations in the present study were inspired by experimental findings demonstrating that the CoM was displaced horizontally with amplitudes greater than those previously recorded for similar forward trunk bending movements (Stapley et al. 1998). These findings led us to verify through the detailed analysis of linear and angular joint displacements, joint torques and CoP displacements if whole body reaching strategies associated with an unchanging horizontal CoM position are feasible. As the human skeleton contains up to 150 degrees of freedom, simulated strategies represented only one from an infinite number of possible limb configurations. Our simulation procedures were nevertheless designed so that angular configurations required to fix the horizontal position of the CoM approached, as closely as possible, those of recorded strategies (see Sect. 2.4). The conservation of experimentally recorded wrist trajectories also meant that simulated trials were compatible with both CoM stabilisation and object grasp.

4.1 Synergies between upper and lower body segments

During experimental and simulated whole body reaching forward horizontal displacements of the head, shoulder and knee opposed backward hip displacements. This is in accordance (except for knee displacements) with patterns of axial synergies seen in forward trunk bending movements (Crenna et al. 1987). However, despite these 'compensatory synergies', experimental CoM displacements were not effectively minimised. Average horizontal CoM amplitudes of between 0.050 m (D1E) and 0.091 m (D2E) greatly exceeded those previously reported (0.010 m) by Crenna et al. (1987). A great deal of evidence supports the theory of CoM position as the stabilised reference value for posture and movement coordination (see Massion 1992). If this theory was assumed to hold true for whole body reaching, greater backward hip displacements should have been recorded when reaching distance increased (resulting in increased wrist and trunk forward displacements). Such a pattern of segmental displacements was seen in simulated but not experimental trials; indeed, backward hip displacements significantly reduced with increasing object distance (see Figs. 4B, D). Trunk angular displacements with respect to the vertical during experimental trials were also similar to those of forward trunk bending. Indeed, Alexandrov et al. (1998) reported average values of $50° \pm 7°$ and as high as $59° \pm 11°$ in three of ten subjects, accompanied by horizontal CoM displacements estimated to be as low as 0.016 ± 0.004 m. This indicates that large forward CoM displacements seen in experimental whole body reaching were not due to greater forward trunk displacements, but arose from the forward displacement of the hip segment with reaching distance. However, it may be argued that a relative forward displacement of the hip with increasing distance of reaching could have resulted from a forward displacement of the ankle marker. Indeed, Fig. 3 shows that this occurred in at least one subject. Thus, further simulations were carried out in order to determine if this was the case by keeping the ankle fixed in space whilst conserving the wrist trajectory. In Appendix 2 and Fig. 9,

we clearly show that slight movement of the ankle forwards is not responsible for a diminution in backward hip displacements with distance.

The body segment configuration under both experimental and simulated conditions was summarised through the analysis of the CoM for upper and lower body segments (Fig. 2). Eng et al. (1992) have shown that the CoM is stabilised by opposing displacements of focal (arm) and lower body (postural) CoM during arm flexion or extension movements. Our experimental results showed that the lower body segments following initial backward displacements (perhaps resulting from the passive action of forward trunk movements) were oriented in a similar direction to both upper and whole body CoM (see Fig. 2). Moreover, only simulated strategies represented what is classically considered as an 'axial synergy' (where CoM displacements are minimised by opposing displacements of focal and postural segments). Thus, in experimental trials, the postural segments did not ensure a strict stabilisation of the body CoM but participated in the focal aspect of reaching movements.

4.2 Experimental versus simulated whole body reaching: the feasibility of keeping the CoM at a constant horizontal position

Simulation procedures have clearly shown that a constancy of the horizontal position of the CoM can be obtained with only slight changes in experimentally recorded body geometry. Indeed, the analysis of simulated angular configurations showed that modifications were required only to shoulder and hip angles, being most pronounced at D2 (see Fig. 5). Differences between mean values of experimental and simulated trials were 4.47° and 1.93° (D1) and 15.7° and 12.7° (D2) for the shoulder and hip, respectively. Ranges of simulated shoulder and hip angular displacements when compared with previously documented anthropometric joint mobility values (Barter et al. 1957) showed that simulated angular displacements (shoulder 49–71.5°, D1 and 73.3–113.3°, D2; hip 73.4–115.8°, D1 and 94.7–143.5°, D2) fell into acceptable ranges for human joint mobility. Thus, angular configurations associated with CoM stabilisation were compatible with object grasp. Moreover, trunk angular displacements with respect to the vertical remained relatively unchanged (61–65°), regardless of the reaching distance or condition. This would indicate that necessary modifications to inter-segmental angles for CoM stabilisation could be made whilst preserving the spatial trunk orientation, previously considered as a primarily controlled variable for balance control (Gurfinkel et al. 1981). The slight modifications to joint angular displacements and thus the physiologically acceptable peaks of individual joint torques could have been expected when considering simulation techniques (least-squares fitting, see Sect. 2.4), but clearly illustrate that if desired, subjects could execute whole body reaching whilst keeping the CoM at the same horizontal position. In light of these findings, what could explain the selection of a strategy of forward CoM displacement rather than its stabilisation during the execution of human whole body reaching?

4.3 Possible explanations for large CoM displacements during human whole body reaching

One explanation is that horizontal CoM displacements permitted the use of gravitational force. During gait initiation (Lepers and Brenière 1995) and more recently whole body reaching (Stapley et al. 1998), APAs have been shown to be centrally programmed to accelerate the CoM forwards. A forward CoM displacement generates an ankle gravitational torque (body mass multiplied by the distance between the CoM and the axis of ankle rotation) which, in turn, accelerates a forward fall. Experimental trials in the present study showed initial forward trajectories of the CoM (Fig. 2). Coupled with ankle net flexor torques, this suggests that whole body reaching may, during its initiation phase, be likened somewhat to an inverted pendulum. Assuming such a configuration, a stabilisation of the CoM (at any position in the BoS) would limit the creation of a moment arm between it and the axis of rotation, and thus prevent the generation and use of an ankle gravitational torque. Indeed, significantly smaller net ankle torques in simulated compared to recorded trials may have resulted from the lack of gravitational torque components.

We also suggest that to conserve the CoM at its initial position excludes the possibility of controlling for disturbing body oscillations during reaching execution. Not only does it prevent the use of the forward foot length as a dynamic equilibrium area, but also limits the control of any destabilisation by the modulation of extensor muscular activity. Clément et al. (1988) have shown that trained acrobats adopted a forward tilt in the upside down standing posture to simplify the control of body oscillations by forearm extensor muscle tone. As the standing posture is generally characterised by a forward body tilt (Gurfinkel 1973), we propose that subjects displace the CoM further forwards during whole body reaching in order to take advantage of soleus or other gastrocnemius muscular activity to control for the disturbing effects of hand trajectory formation or forward trunk displacements.

Finally, stabilising the CoM may imply similar conditions to a reduction in support surface length. Horak and Nashner (1986) have shown that, when on a narrow support surface, postural responses to unexpected horizontal translations switch from 'ankle' strategies (controlling body oscillations by the ankle joint musculature), to 'hip' strategies (compensation at the hip joint). Simulation procedures modified compensatory synergies so that greater backward hip linear and angular displacements characterised strategies where the CoM remained at the same horizontal position. Nevertheless, simulated joint torques (without horizontal CoM displacements) demonstrated similar patterns to those recorded experimentally (see Fig. 6

and Table 2). It is important to note, however, that peak ankle flexor and extensor torques greatly decreased. As a high flexing or extending ankle torque can only be exerted if the CoP is placed close to the toes or heels (and ankle torque directly determines CoP position, Okada and Fujiwara 1984), we suggest that stabilising the CoM at its initial position may limit the production of an external moment for the backward angular momentum required during subsequent lifting movements (see Toussaint et al. 1995). Thus, our results indicate that the control of ankle torque (an ankle strategy) may take precedence over a body configuration necessary for CoM stabilisation (a hip strategy).

4.4 Implications for the integrated control of posture and movement

During whole body reaching, the CNS has to overcome constraints of correct hand trajectory formation and the maintenance of equilibrium. Our simulations have shown it possible to perfectly satisfy these two constraints. This would exclude the possibility that large forward CoM displacements recorded during experimental trials occurred as a necessity of the task, but rather were the result of strategic choice. Until now, explanations have been forwarded to explain only why the CNS might want to stabilise the CoM position during multi-joint movements. When movements involve more than two segments, an identical trajectory of the distal end point may imply an infinite number of segment paths (Soechting and Flanders 1991). Thus, it is assumed that to solve the problem of redundancy, the CNS can reduce but not eliminate the number of redundant degrees of freedom (Bernstein 1967), which may be achieved by stabilising the trunk or CoM (Alexandrov et al.1998; Tyler and Hazan 1995). This study has shown, however, that if this redundancy problem exists during whole body reaching, it is not solved by stabilising the CoM as subjects did not choose this feasible strategy. Further study will be undertaken to investigate the manner in which the CNS overcomes the problem of redundant degrees of freedom during whole body reaching by investigating possible coupling of joint angles in CoM free and stabilised movements.

The present findings cast doubt upon the theory of the CoM as the stabilised reference value whose displacements are minimised by axial synergies. This has important implications for the central control of posture and movement coordination, described by Massion (1992, 1994) to be characterised by separate pathways. Experimental whole body reaching showed that postural segments (hip) also participated in the focal aspect of the movement. This may go some way to illustrating a common central command controlling both goal-directed movements and associated postural adjustments. It is clear from our results that in a task such as whole body reaching, the distinction between focal (those that perform the voluntary movement) and postural segments (those that provide the necessary associated postural adjustments) cannot be made, but rather that there is some higher integration of postural control and movement coordination.

Acknowledgements. This work was supported by grants from the Centre National d'Etudes Spatiaes (CNES). We thank Dr AJ Van Soest for his helpful comments on an earlier version of the manuscript.

Appendix 1

Angles θ, fitting (6), and supplying minimum values to square functions (7) were calculated using iteration procedures. Calculations were performed for each 10-ms time frame. The set of angles θ, obtained after the ith iteration is denoted by the vector θ^i. Thus, components of the starting vector θ^0 are equal to recorded values $\tilde{\theta}$. In order to find angles θ for the ith iteration step, the system (6) is replaced with its linear approximation as follows:

$$\begin{cases} X_{\mathrm{wr}}(\theta^{i-1}) + \sum_{j=1}^{6} (\theta_j^i - \theta_j^{i-1}) \partial X_{\mathrm{wr}} / \partial \theta_j = \tilde{X}_{\mathrm{wr}} \\ Y_{\mathrm{wr}}(\theta^{i-1}) + \sum_{j=1}^{6} (\theta_j^i - \theta_j^{i-1}) \partial Y_{\mathrm{wr}} / \partial \theta_j = \tilde{Y}_{\mathrm{wr}} \\ X_{\mathrm{CM}}(\theta^{i-1}) + \sum_{j=1}^{6} (\theta_j^i - \theta_j^{i-1}) \partial X_{\mathrm{CM}} / \partial \theta_j = \tilde{X}_{\mathrm{CM}} \ . \end{cases} \tag{9}$$

$\boldsymbol{U}$ and $\boldsymbol{V}$ can be denoted by the following vectors:

$$U = \left\| \theta_1^i - \theta_1^{i-1}, \theta_3^i - \theta_3^{i-1}, \theta_5^i - \theta_5^{i-1} \right\|^* \quad \text{and}$$
$$V = \left\| \theta_2^i - \theta_2^{i-1}, \theta_4^i - \theta_4^{i-1}, \theta_6^i - \theta_6^{i-1} \right\|^* \ ,$$

the sign * denoting transposition. Using these notations, the system (5) can be written as:

$$\mathbf{A}U + \mathbf{B}V = D \tag{10}$$

where $\mathbf{A}$ and $\mathbf{B}$ = matrices of corresponding partial derivatives, $\boldsymbol{D}$ = a vector:

$$D = \left\| \tilde{X}_{\mathrm{wr}} - X_{\mathrm{wr}}(\theta^{i-1}), \tilde{Y}_{\mathrm{wr}} - Y_{\mathrm{wr}}(\theta^{i-1}), X_0 - X_{\mathrm{CM}}(\theta^{i-1}) \right\|^* \ .$$

During whole body reaching movements, the body configuration was such that the matrix $\mathbf{A}$ could be inverted, thus:

$$U = \mathbf{A}^{-1} D - \mathbf{A}^{-1} \mathbf{B} V. \tag{11}$$

This is an expression of vector $\boldsymbol{U}$ with three unknown parameters; components of the vector $\boldsymbol{V}$, matrices **A, B** and the vector $\boldsymbol{D}$ are known at the $\boldsymbol{i}$th step iteration.

Thus, the function $\boldsymbol{S}(4)$ can be written as:

$$S = \sum_{j=1}^{3} (U_j - \tilde{U}_j)^2 + \sum_{j=1}^{3} (V_j - \tilde{V}_j)^2 \tag{12}$$

where

$$\tilde{U} = \left\| \tilde{\theta}_1 - \theta_1^{i-1}, \tilde{\theta}_3 - \theta_3^{i-1}, \tilde{\theta}_5 - \theta_5^{i-1} \right\|^*$$

and

$$\tilde{V} = \left\| \tilde{\theta}_2 - \theta_2^{i-1}, \tilde{\theta}_4 - \theta_4^{i-1}, \tilde{\theta}_6 - \theta_6^{i-1} \right\|^* \ .$$

As the components of the vector $\mathbf{V}$ are independent parameters, at the minimum point of the function $\boldsymbol{S}$, the partial derivatives $\partial S / \partial V_l$ should equal zero:

$$2 \sum_{j=1}^{3} (U_j - \tilde{U}_j) \partial U_j / \partial V_l + 2(V_l - \tilde{V}_l) = 0 \quad l = 1, 2, 3 \tag{13}$$

Using (7), the derivative $\partial U_j/\partial V_l$ can be expressed as $-(\mathbf{A}^{-1}\mathbf{B})_{jl}$ or $\partial U_j/\partial V_l = -(\mathbf{A}^{-1}\mathbf{B})^*_{lj}$. Therefore, (9) can be transformed to:

$$(\mathbf{A}^{-1}\mathbf{B})^*\mathbf{A}^{-1}\mathbf{B}V + V = (\mathbf{A}^{-1}\mathbf{B})^*\mathbf{A}^{-1}D - (\mathbf{A}^{-1}\mathbf{B})^*\tilde{U} + \tilde{V} \ . \qquad (14)$$

The vector equation (10) consists of a system of three scalar linear equations. In solving this system, all three components of the unknown vector **V** can be obtained. Following this, the vector **U** can be calculated using (7). This successfully gives the set of angles θ^i after the ith iteration. The whole procedure is repeated until each component of vector **D** achieves an absolute value inferior to an acceptable threshold. The above algorithm was numerically implemented using the algorithmic language Pascal.

Appendix 2

Figure 9 shows a comparison for one typical subject between recorded whole body reaching movements (where the ankle could marker could displace forwards) and simulated whole body reaching where the ankle marker was fixed in space (whilst conserving an identical wrist trajectory). The figure shows that the difference between the two strategies (ankle free, ankle fixed) had a negligible effect upon whole body angular configuration (differences were greatest at D2N). Most importantly, however, this simulation proved that any slight forward displacement of the ankle marker during reaching does not account for a smaller backward displacement of the hip marker with increasing distance.

References

Alexandrov A, Frolov A, Massion J (1998) Axial synergies during human upper trunk bending. Exp Brain Res 118:210–220

Babinski J (1899) De l'asymmetrie cérébelleuse. Rev Neurol (Paris) 7:806–816

Barter JT, Emmanuel I, Truet B (1957) A statistical evaluation of joint range data. WADCTR 57311, Wright-Patterson Air Force Base, Ohio. In: Chaffin B, Andersson G (eds) Occupational biomechanics. Wiley, New York, pp 86–87

Belenkii YY, Gurfinkel V, Paltsev Y (1967) Elements of control of voluntary movements. Biofizika 12:135-141

Bernstein N (1967) The coordination and regulation of movements. Pergamon, Oxford

Bouisset S, Zattara M (1981) A sequence of postural movements precedes voluntary movement. Neurosci Lett 22:263–270

Bouisset S, Zattara M (1987) Biomechanical study of the programming of anticipatory postural adjustments associated with voluntary movement. J Biomech 20:735–742

Clément G, Pozzo T, Berthoz A (1988) Contribution of eye positioning to control of the upside-down standing posture. Exp Brain Res 73:569–576

Cordo P, Nashner LM (1982) Properties of postural adjustments associated with rapid arm movements. J Neurophysiol 47:287–302

Crenna P, Frigo C, Massion J, Pedotti A (1987) Forward and backward axial synergies in man. Exp Brain Res 65:538–548

Eng JJ, Winter DA, MacKinnon CD, Patla AE (1992) Interaction of the reactive moments and centre of mass displacement for postural control during voluntary arm movements. Neurosci Res Commun 11:73–80

Friedli WG, Hallet M, Simon SR (1984) Postural adjustments associated with rapid voluntary arm movements. 1. Electromyographic data. J Neurol Neurosurg Psychiatry 47:611–622

Gurfinkel VS (1973) Muscle afferentiation and postural control in man. Agressologie 14:1–8

Gurfinkel VS, Lipshits MI, Mori S, Popov KE (1981) Stabilisation of body position as the main task of postural regulation. Fiziol Chel 7:400–410

Horak FB, Nashner LM (1986) Central programming of postural movements: adaptation to altered support-surface configurations. J Neurophysiol 55:1369–1381

Horstmann GA, Dietz V (1990) A basic posture control mechanism: the stabilisation of the centre of gravity. Electroencephalogr Clin Neurophysiol 76:165–176

Kingma I, Toussaint HM, Commissaris DACM, Hoozemans MJM, Ober MJ (1995) Optimizing the determination of the body center of mass. J Biomech 28:1137–1142

Lee WA, Buchanan TS, Rogers MW (1987) Effects of arm acceleration and behavioral conditions on the organization of postural adjustments during arm flexion. Exp Brain Res 66:257–270

Lepers R, Brenière Y (1995) The role of anticipatory postural adjustments and gravity in gait initiation. Exp Brain Res 107:118–124

Massion J (1992) Movement, posture and equilibrium: interaction and coordination. Prog Neurobiol 38:35–56

Massion J (1994) Postural control system. Curr Opin Neurobiol 4:877–887

Massion J, Popov K, Fabre JC, Rage P, Gurfinkel VS (1997) Is the erect posture in microgravity based on the control of trunk orientation or center of mass position? Exp Brain Res 114:384–389

Mouchnino L, Aurenty R, Massion J, Pedotti A (1992) Coordination between equilibrium and head-trunk orientation during leg movement: a new strategy built up by training. J Neurophysiol 67:1587–1598

Mouchnino L, Cincera M, Fabre JC, Assaiante C, Amblard B, Pedotti A, Massion J (1996) Is the regulation of the center of mass maintained during leg movement under microgravity conditions? J Neurophysiol 76:1212–1223

Nardone A, Schiepatti M (1988) Postural adjustments associated with voluntary contraction of leg muscles in standing man. Exp Brain Res 69:469–480

Oddsson L (1988) Coordination of a simple voluntary multi-joint movement with postural demands: trunk extension in standing man. Acta Physiol Scand 134:109–118

Oddsson L, Thortensson A (1986) Fast voluntary trunk flexion movements in standing: primary movements and associated postural adjustments. Acta Physiol Scand 140 [Suppl 595]:1–60

Okada M, Fujiwara K (1984) Relation between sagittal distribution of the foot pressure in upright stance and relative EMG magnitude in some leg and foot muscles. J Hum Ergol 13:97–105

Pedotti A, Crenna P, Deat A, Frigo C, Massion J (1989) Postural synergies in axial movements: short and long term adaptation. Exp Brain Res 74:3–10

Plagenhoef S, Gaynor Evans FG, Abdelnour T (1983) Anatomical data for analyzing human motion. Res Q Exerc Sport 54:169–178

Ramos CF, Stark LW (1990a) Postural maintenance during movement: simulations of a two joint model. Biol Cybern 63:363–375

Ramos CF, Stark LW (1990b) Postural maintenance during fast forward bending: a model simulation experiment determines the 'reduced trajectory'. Exp Brain Res 82:651–657

Soechting JF, Flanders M (1991) Arm movements in three dimensional space: computation, theory and observation. Exerc Sport Sci Rev 19:389–418

Stapley P, Pozzo T, Grishin A (1998) The role of anticipatory postural adjustments during whole body forward reaching movements. NeuroReport 9:395–401

Toussaint H, Commissaris DACM, Dieën JH van, Reijnen JS, Praet SFE, Beek PJ (1995) Controlling the ground reaction force during lifting. J Mot Behav 27:225–234

Tyler AE, Hazan Z (1995) Qualitative discrepancies between trunk muscle activity and dynamic postural requirements at the initiation of reaching movements performed while sitting. Exp Brain Res 107:87–95